

## Controlling synoptic-scale factors for the distribution of transient luminous events

Li-Jou Lee,<sup>1</sup> Alfred B. Chen,<sup>2,3</sup> Shu-Chun Chang,<sup>1</sup> Cheng-Ling Kuo,<sup>4,5</sup> Han-Tzong Su,<sup>1,5</sup> Rue-Rou Hsu,<sup>1,2,5</sup> Chun-Chieh Wu,<sup>6</sup> Po-Hsiung Lin,<sup>6</sup> Harald U. Frey,<sup>7</sup> Stephen B. Mende,<sup>7</sup> Yukihiro Takahashi,<sup>8</sup> and Lou-Chuang Lee<sup>4</sup>

Received 1 September 2009; revised 25 February 2010; accepted 10 March 2010; published 25 August 2010.

[1] From analyzing the distribution of the transient luminous events (TLEs) registered by the Imager of Sprites and Upper Atmospheric Lightning payload on the FORMOSAT-2 satellite, we deduced the synoptic-scale factors that control the occurrence of TLEs. For the low-latitude tropical regions (25°S ~ 25°N), 84% of the TLEs were found to occur over the Intertropical Convergence Zone and the South Pacific Convergence Zone and exhibited a seasonal variation that migrates north and south with respect to the equator. For the midlatitude regions (latitudes beyond ±30°), the occurrence of TLEs congregated over the Pacific Ocean, the Atlantic Ocean, and the Mediterranean Sea during the winter seasons. From studying the distributions of the daily winter storm centers and the winter TLEs, the winter TLEs are usually found to occur near the cold fronts and thus are closely related to the winter storms. Our study shows that 88% of the northern winter TLEs and 72% of the southern winter TLEs occurred near the midlatitude cyclones. The winter TLE occurrence density and the storm-track frequency share similar trends with the distribution of the winter TLEs offset by 10°–15°. Additionally, this study compares the luminous intensities of elves and sprites from the tropical and winter midlatitude regions. The results show that the convective systems in the tropical regions are presumably more capable of producing bright TLEs in comparison to their winter counterparts.

**Citation:** Lee, L.-J., et al. (2010), Controlling synoptic-scale factors for the distribution of transient luminous events, *J. Geophys. Res.*, 115, A00E54, doi:10.1029/2009JA014823.

### 1. Introduction

[2] It has been 20 years since the recording of the first sprite in 1989 [Franz et al., 1990]. In the past two decades, transient luminous events (TLEs) have been observed in many geographic locations around the world: North and South America [Lyons, 1996; São Sabbas and Saba, 2008; Sentman et al., 1995; van der Velde et al., 2007], the Mediterranean Sea

[Yair et al., 2009; Yano et al., 2001], Europe [Neubert et al., 2001], Australia [Hardman et al., 2000], Japan [Fukunishi et al., 1996; Takahashi et al., 2003], and the Asian continent [Hsu et al., 2003; Su et al., 2002, 2003; Yang et al., 2008]. These observations testify that TLEs are a global phenomenon. From analyzing Imager of Sprites and Upper Atmospheric Lightning (ISUAL) recorded events, Chen et al. [2008] have deduced the global TLE distributions and the occurrence rates. The TLEs observed from various areas and in various seasons are produced by different regional weather systems. For example, the weather systems that induced the winter sprites in Japan [Adachi et al., 2005] and the Mediterranean Sea [Ganot et al., 2007] are cold fronts or cold air masses, whereas the sprites over the summer U.S. high plains [Lyons, 1996] are initiated by mesoscale convective systems (MCSs). However, the causes behind these TLE distributions remain to be clarified. Between July 2004 and August 2008, ISUAL payload on the FORMOSAT-2 satellite registered about ten thousand TLEs. Figure 1 shows the global distributions of the ISUAL TLEs for the northern summers and winters in this period. The maps indicate that there are distinct groups of TLEs: the tropical groups over the low-latitude regions and the winter groups over the midlatitude regions. In this article, the synoptic-scale factors that affect the TLE distributions in the low-latitude tropical

<sup>1</sup>Department of Physics, National Cheng Kung University, Tainan, Taiwan.

<sup>2</sup>Institute of Space, Astrophysical and Plasma Sciences, National Cheng Kung University, Tainan, Taiwan.

<sup>3</sup>Plasma and Space Science Center, National Cheng Kung University, Tainan, Taiwan.

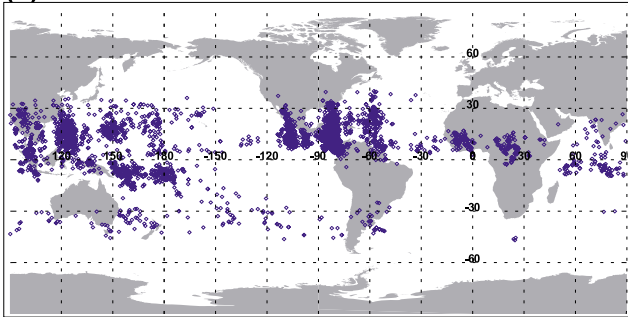
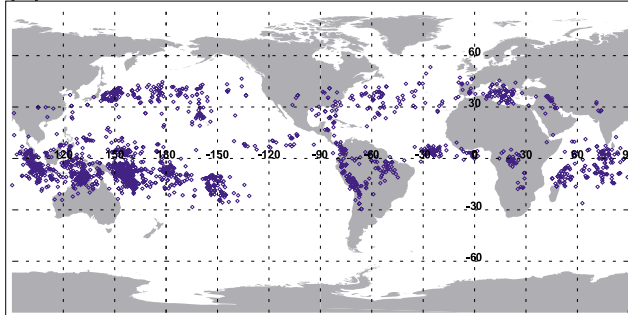
<sup>4</sup>Institute of Space Science, National Central University, Zhongli, Taiwan.

<sup>5</sup>Earth Dynamic System Research Center, National Cheng Kung University, Tainan, Taiwan.

<sup>6</sup>Department of Atmospheric Sciences, National Taiwan University, Taipei, Taiwan.

<sup>7</sup>Space Sciences Laboratory, University of California, Berkeley, California, USA.

<sup>8</sup>Department of CosmoSciences, Hokkaido University, Sapporo, Japan.

**(a) Northern summers****(b) Southern summers**

**Figure 1.** Global distributions of ISUAL TLEs for (a) the northern summers (June to August) and (b) the southern summers (December to February).

(25°S ~ 25°N) and the midlatitude winter (beyond  $\pm 30^\circ$ ) regions are explored. The luminous intensities of the TLEs from the tropical and winter regions are also compared.

## 2. Instruments and Data Sets

[3] ISUAL is the scientific payload on the FORMOSAT-2 satellite that moves along a Sun-synchronized orbit at 891 km altitude [Chern *et al.*, 2003]. The ISUAL payload contains three sensors: an intensified CCD imager, a six-channel spectrophotometer (SP), and a dual-module array photometer (AP). The imager and SP are coaligned to look at the same direction, and their fields of view (FOVs) are  $20^\circ(\text{H}) \times 5^\circ(\text{V})$ . The imager took the TLE images reported in this work through a ( $\text{N}_2$  first positive band  $\text{N}_2 1\text{P}$ , 623–750 nm) filter and with a frame integration time of 29 ms. The time resolution of the ISUAL SP is 0.1 ms, and the SP channels include SP1 (far-ultraviolet, FUV; 150–290 nm), SP2 (centered at 337 nm), SP3 (centered at 391 nm), SP4 (658.9–753.4 nm), SP5 (centered at 777.4 nm), and SP6 (middle-ultraviolet, MUV; 250–390 nm). The AP consists of dual 16-anode arrays, the blue module (370–450 nm) and the red module (530–650 nm); each module has a combined FOV of  $22^\circ(\text{H}) \times 3.6^\circ(\text{V})$ . ISUAL is configured with an eastward limb view and to detect TLEs that occur near the local midnight. The geolocation uncertainty of a TLE is  $\sim 50$  km/pixel in the latitudinal direction and 50 ~ 220 km longitudinally [Chen *et al.*, 2008]. For the northern summers, the ISUAL survey region covers 45°S–25°N latitudes. While for the northern winters, the ISUAL surveyed zone shifts to 25°S–45°N latitudes. The South Atlantic anomaly region was usually excluded from the

ISUAL survey to minimize the damages that the energized instruments might have incurred from the influx of the high-energy particles. The hourly average occurrence of intense lightning over continent and ocean at this local time is comparable to the diurnal mean as reported by Füllekrug [2004]. Therefore, the TLE rates deduced from the ISUAL data likely are not biased by this restricted observation window.

[4] Besides the ISUAL data, three additional sets of meteorological data are also used in this work. The outgoing longwave radiation (OLR) monthly data from the National Oceanic and Atmospheric Administration (NOAA) and the longitudinal/latitudinal wind field (u/v wind) at 200 hPa height from National Centers for Environmental Prediction/National Center for Atmospheric Research (NCEP/NCAR) Reanalysis are used to define the Intertropical Convergence Zone (ITCZ) and the South Pacific Convergence Zone (SPCZ) (section 3.1). The four-times-daily data at sea-level pressure (SLP) from NCEP/NCAR Reanalysis are used to define the centers of the midlatitude cyclones (section 4.2). For these sets of meteorological data, the spatial resolution is  $2.5^\circ$  latitude  $\times$   $2.5^\circ$  longitude.

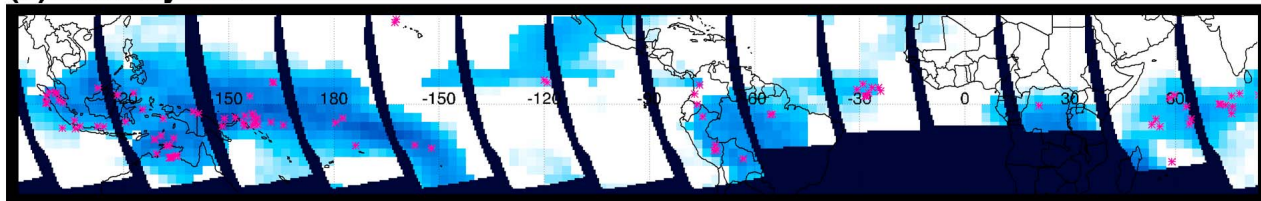
## 3. Low-Latitude Tropical TLEs

[5] For the low-latitude tropical regions, the distributions of TLEs exhibit seasonal variation patterns that migrate north and south with respect to the equator. ITCZ is the convergence zone of the interhemisphere trade winds [Hu *et al.*, 2007], and SPCZ is linked to the ITCZ in the west Pacific warm pool that stretches southeastward [Ortega and Guignes, 2007]. The ITCZ and SPCZ not only contain strong convective cloud systems and heavy precipitation but also show seasonal migrating patterns that are similar to those for the TLEs. The similarity in the migration patterns between TLEs and the ITCZ and SPCZ motivates us to initiate this study to further investigate the relation between the seasonal migration of the TLE distributions and the movement of the ITCZ and SPCZ.

### 3.1. Correlating the TLE and the ITCZ/SPCZ Distributions

[6] The OLR data are used to define the distribution of the ITCZ and SPCZ, which in turn represent the distribution of the tropical convective systems. For regions having lower OLR value, they either have lower surface temperatures or are shielded by deep convective cloud systems. However, if the OLR value for a region is less than the clear-sky OLR background ( $OLR_b$ ), then this area is surely covered by the convective cloud. Hence the  $OLR_b$  was taken as a threshold value to screen out the regions of the ITCZ and SPCZ. The  $OLR_b$  so defined is based on the surface temperature and the clear-sky greenhouse effect as reported by Gu and Zhang [2002]. Using the empirical equation of Gu and Zhang [2002], the  $OLR_b$  value is calculated to be  $270 \text{ W/m}^2$  when the average minimum surface temperature of the tropical region (25°S ~ 25°N) is taken to be  $20^\circ\text{C}$  as that in the NOAA data. Hence, the general ITCZ and SPCZ are the tropical regions whose OLR values are less than  $270 \text{ W/m}^2$ . To check whether a region conforms to the characteristics of ITCZ and SPCZ, in this region the winds have to converge near the ground but diverge at the higher levels. Since the error in deducing the horizontal wind field

## (a) January 2007



## (b) July 2007

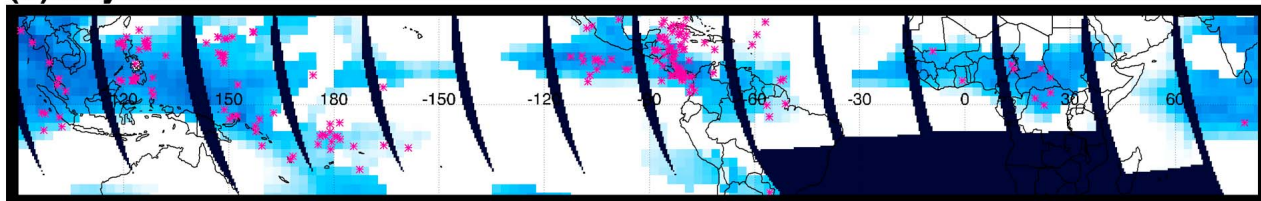


**Figure 2.** Distributions of the ISUAL TLEs and the ITCZ in January 2007 and July 2007. The blue-shaded areas around the equator are the ITCZ, and that stretching from the west Pacific to the southeast Pacific is the SPCZ. The red crosses represent ISUAL TLEs, and the black stripes are unsurveyed regions of the ISUAL experiment.

is higher at low levels than at higher levels, the higher-level value is used in this study. The divergence field equation at 200 hPa height can be defined from the longitudinal wind field ( $u$ ) and the latitudinal wind field ( $v$ ):  $\nabla \cdot \bar{V}_{200\text{hPa}} = \frac{\partial u}{\partial x} + \frac{\partial v}{\partial y}$ , where  $x$  and  $y$  are the longitudinal and the latitudinal coordinates, respectively. The condition  $\nabla \cdot \bar{V}_{200\text{hPa}} > 0$  represents that the winds diverge at higher levels and is considered as a more useful filter in finding the ITCZ/SPCZ regions. In summary, the ITCZ and SPCZ defined in this work are the regions having OLR values less than  $OLR_b$  ( $270 \text{ W/m}^2$ ) and  $\nabla \cdot \bar{V}_{200\text{hPa}}$  greater than 0.

[7] Figure 2 shows the distributions of TLEs and ITCZ/SPCZ in January 2007 and July 2007. The red crosses represent the ISUAL TLEs, the blue shaded areas around the equator are the ITCZ, that stretching over the west Pacific to the southeast Pacific are the SPCZ, and the black stripes are ISUAL unsurveyed regions. Figure 2 indicates that most of the ISUAL TLEs occurred over the ITCZ and SPCZ. In January the ITCZ is mostly distributed to the south, and most of the TLEs also occurred over the south of the equator. While in July, the ITCZ migrated north and so did the TLE distribution. From July 2004 to August 2008, ISUAL recorded 8347 TLEs that occurred between  $25^\circ\text{S}$  and  $25^\circ\text{N}$ , and 7018 of them occurred in the regions with  $\nabla \cdot \bar{V}_{200\text{hPa}} > 0$ . Figure 3 shows the binned distribution of the OLR values for the 7018 tropical TLEs, where 84% of TLEs occurred over the regions having OLR smaller than  $OLR_b$  and  $\nabla \cdot \bar{V}_{200\text{hPa}}$  greater than 0. This means that 84% of the recorded tropical TLEs occurred over the ITCZ and SPCZ. However, the OLR value used in this work to locate the ITCZ/SPCZ region is a monthly average value. Therefore, the other 16% of ISUAL TLEs still could have been induced by short-lived or regional convective systems, whose regions were not classified as ITCZ/SPCZ after averaging.

### 3.2. Migrating Characteristics in the Distributions of TLEs and ITCZ

[8] *Waliser and Gautier* [1993] and *Hu et al.* [2007] indicate that the distribution and seasonal migration characteristics of ITCZ vary among different longitudinal domains. To discern whether the migrating characteristics of the tropical TLEs and the ITCZ are the same, we divided the surface region of the Earth into eight longitudinal domains (Table 1), as suggested by *Waliser and Gautier* [1993]. There are no ISUAL data for December 2004, January 2005, and

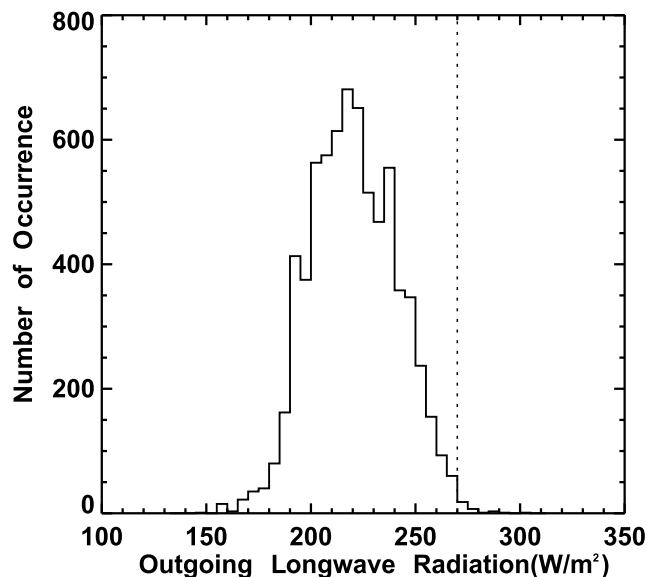


**Figure 3.** The OLR histogram for the 7018 tropical ISUAL TLEs that occurred in the regions with divergent  $\nabla \cdot \bar{V}_{200\text{hPa}} > 0$ . The dashed line denotes the  $OLR_b = 270 \text{ W/m}^2$ .

**Table 1.** Eight Longitudinal Domains and Their Boundaries

Domain	Longitude Limits
Global	0° ~ 360°
Africa	0° ~ 45°
Indian Ocean	45° ~ 105°
West Pacific Ocean	105° ~ 150°
Central Pacific Ocean	150° ~ 240°
East Pacific Ocean	240° ~ 280°
South America	280° ~ 315°
Atlantic Ocean	315° ~ 360°

April 2005. Thus, to obtain more accurate annual TLE distribution characteristics, the data between September 2005 and August 2008 are used. Figure 4 shows the monthly variation of the latitudinal ISUAL TLE distributions and the annual cycles of ITCZ reported by *Waliser and Gautier* [1993] for the eight chosen longitudinal domains. Note that the domain from the east coast of South America to South Africa contains the South Atlantic anomaly (SAA) region. ISUAL carried out only limited campaigns in the SAA region, and the cumulative observation time is low. Therefore, the TLE variation characteristics over the Africa, South America, and Atlantic domains may have larger errors than those over other domains.

[9] The annual global latitudinal TLE distribution is nearly sinusoidal, as shown in Figure 4a. The distribution of the ISUAL TLEs reaches the most northern latitude in July and August, while it reaches the most southern latitude in February and March. The distribution characteristic of TLEs is similar to that of the ITCZ, since both are expected to reflect the effect of the solar radiation cycle. Figure 4b shows that the TLEs are few in the region of 20°N–25°N over the African Sahara desert, which is a region known to have few convective systems. For the domain over the Indian Ocean (Figure 4c), the latitudinal migrating range of the TLE distribution is relatively large and varies from ~20°S to 25°N. In addition, the TLE distribution for this domain seems to segregate into two bands during the northern summers: the southern India (12°N–25°N) band and a band near the equator (6°S–7°N). The annual TLE distribution over the western Pacific Ocean (Figure 4d) also has a sinusoidal feature. The TLE distribution for this domain is more symmetrical compared to that for the Indian Ocean. For the central Pacific Ocean (Figure 4e), the TLE distribution is composed of northern and southern zones straddling the equator; the more numerous TLEs in the southern zone were induced by the strong convective systems in the SPCZ. Almost all the TLEs over the east Pacific Ocean (Figure 4f) occurred north of the equator. The southeast Pacific Ocean is under the influence of the ocean current from the polar region, and the sea surface temperature is lower than that in other Pacific Ocean regions. In addition, the southeast Pacific Ocean area also is a downdraft region of the longitudinal atmospheric circulation, so the convective systems are normally hard to form. For the South America domain (Figure 4g), the annual TLE distribution is also near sinusoidal. The TLE distribution over the Atlantic Ocean domain (Figure 4h) shows that it reaches the most northern latitude, 20°N, in July and August.

[10] Comparing the annual cycles of the TLEs and the ITCZ in Figure 4, the curves match well for the global, Indian

Ocean, and Atlantic Ocean domains (Figures 4a, 4c, and 4h). While for the Africa, west Pacific, east Pacific, and South America domains (Figures 4b, 4d, 4f, and 4g), the cycle periods of the TLEs and the ITCZ are consistent, but deviations exist between the most northern and the most southern latitudes of the TLEs and the ITCZ cycles. For the Africa domain (Figure 4b), the cumulative ISUAL observation time is low over the South Africa region, which may have contributed to the notable deviation for the TLEs and the ITCZ cycles over the southern region. For the west Pacific domain (Figure 4d), the tropical cyclones are frequently occurring phenomena in southeastern Asia during the northern summer and in the north of Australia during the southern winter. The tropical cyclones are severe weather systems that are known to induce recursive TLEs from the same region [*Tsai*, 2008]; hence the TLE cycle may contain more pronounced peaks and thus deviates substantially from the ITCZ peaks in this region. For the South America (Figure 4g) and east Pacific (Figure 4f) domains, the tropical cyclones also often rampage through the Caribbean Sea during the northern summer; these severe weather systems may have also induced a fair amount of TLEs and caused the deviation between the TLEs and the ITCZ cycles. As for the east Pacific Ocean in northern winter, the TLEs and the ITCZ data are both sparse owing to undersampling, and the deviation may not be real. In summary, the migrating characteristics of the TLE distributions for the eight longitudinal domains vary but closely follow those of the ITCZ.

#### 4. Occurrence of Winter TLEs

[11] Northern midlatitude regions are excluded from the ISUAL survey during the northern summers, since the ISUAL low-light-level instruments have to be turned off before exiting the eclipse near 30°N. The same situation is also applied for the southern midlatitude regions during the southern summers. Therefore, for the midlatitude regions, only the TLEs recorded by ISUAL in their winter seasons are analyzed. During the northern winters, the occurrence of TLEs increases and congregates over some specific regions, more notably over the Mediterranean Sea, the east coast of Japan to the central Pacific Ocean, and the east coast of North America to the Atlantic Ocean. During the southern winters, TLEs occur frequently over the region stretching from the east and the south coasts of Australia to the southern Pacific Ocean and over the southeast coast of South America.

[12] From ground observations, winter TLEs were found to be associated with the passing of the cold fronts [*Takahashi et al.*, 2003]. As an illustrative case, ISUAL recorded three elves, three sprites, and two halos over the west Pacific Ocean on 2 December 2005. Figure 5 shows the weather map for the surveyed region at the time of the TLEs, courtesy of the Japan Meteorological Agency. From the weather map, it can be discerned that the observed winter TLEs (Figure 5, red crosses) occurred near the cold front or, more exactly, near the cold front of the “midlatitude cyclone.” Therefore, in sections 4.1 and 4.2, we always correlate the winter TLEs with the midlatitude cyclones instead of the cold fronts.

##### 4.1. Winter TLEs and Midlatitude Cyclone Centers

[13] A cold front is one of the most prominent structures of the midlatitude cyclones, and the weather of this region

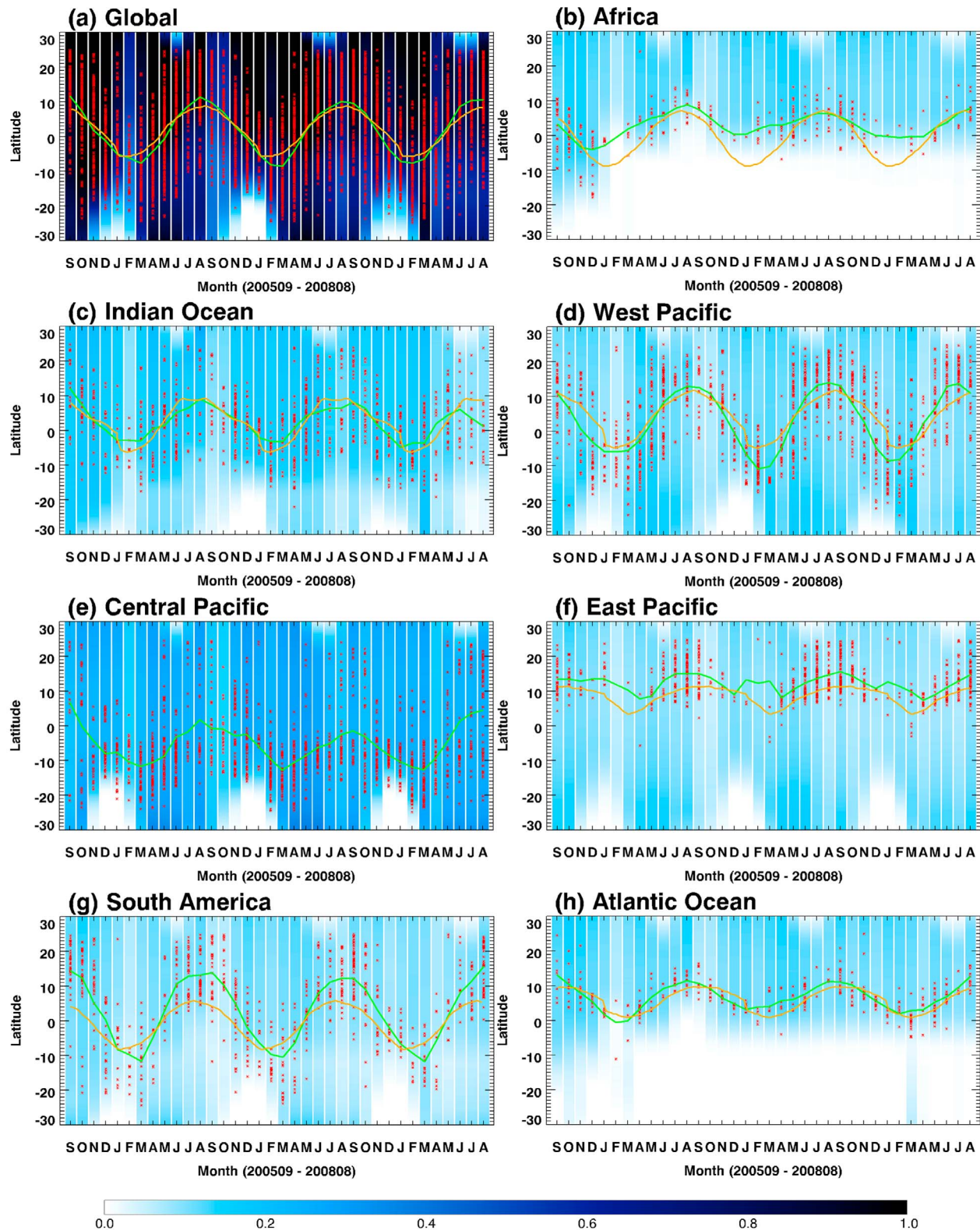


**Figure 4.** (a–h) The monthly variation of TLE distributions and the annual cycles of ITCZ for the eight domains. The  $x$  axis denotes the month in a year from September 2005 to August 2008, the  $y$  axis denotes the occurrence latitudes of TLEs, the red crosses represent the TLEs, and the green curves are the spline fits to the TLE distributions. The blue shading in the background represents the cumulative ISUAL observation time in this latitude; darker shade means longer observation time. The local observation time is normalized to the total cumulative observation time. The orange curves are the annual cycles of ITCZ distribution reported by *Waliser and Gautier* [1993].

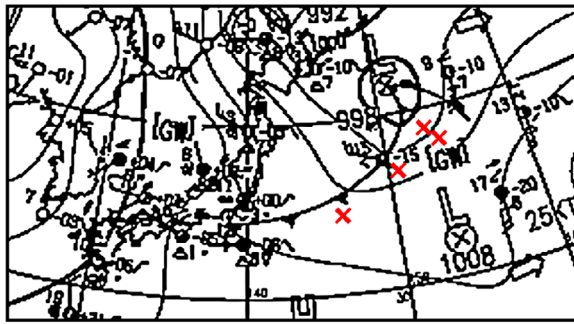


**Figure 5.** Winter TLEs recorded in the western Pacific Ocean on 2 December 2005. The weather map is obtained from the Japan Meteorological Agency, and the red crosses represent the locations of the winter TLEs.

in the winter is seriously affected by the passing of these midlatitude cyclones. To study the correlation of winter TLEs and midlatitude cyclones, we compare the locations of winter TLEs and the midlatitude cyclone centers. We use the 6 hour SLP grid data to locate the midlatitude cyclone centers as suggested by *Eichler and Higgins* [2006] and *Serreze et al.* [1997]. The midlatitude cyclone centers are identified by finding the local minimum of the SLP and are rechecked to make certain that the SLP values are less than 1000 hPa and are at least 1 hPa lower than their surrounding grids.

[14] In the winter, the low-pressure centers are usually formed near the eastern coast of a continent and then move east toward the warmer ocean in the westerly belt. The warm ocean surface supplies the energy to the low pressures to develop into midlatitude cyclones. The development and the tracing characteristics of the midlatitude cyclones can be inferred from the daily SLP data. To correlate the winter TLEs and the midlatitude cyclones, the winter TLEs are plotted on the same interval daily SLP map for the midlatitude cyclones. If a winter TLE occurs in the region between the midlatitude cyclone center and the 1015 hPa isobaric line, then it counts as having correlation with the midlatitude cyclone. Between July 2004 and August 2008, in the midlatitude regions (greater than  $\pm 30^\circ$ ), ISUAL recorded 312 winter TLEs during the northern winters and 127 winter TLEs during the southern winters. For the northern winter

regions, the results indicate that the occurrence of the winter TLEs follows the eastward movement of the midlatitude cyclones and concentrates over three main areas, the Pacific Ocean, the Atlantic Ocean, and the Mediterranean Sea, through correlating the daily winter TLEs with the SLP maps. The midlatitude cyclones over the Pacific Ocean tend to be large in size, form around Japan, and then gradually develop the eastward tracing. Most of the observed winter TLEs occurred to the south of the midlatitude cyclone centers and are often distributed along a line south of the cyclones (Figure 6a). The sizes of the midlatitude cyclones in the Atlantic Ocean are smaller than those over the Pacific Ocean. However, the winter TLEs are still located to the south of the cyclones, but the event number was less and the distribution was more scattered (Figure 6b). The midlatitude cyclones over the Mediterranean Sea usually originate over southern Europe and northern Africa. Since the area of the Mediterranean Sea is much smaller than that of the Pacific and Atlantic Oceans, the size of the midlatitude cyclones are the smallest among the trio (Figure 6c). However, the eastward track feature is shared by all the midlatitude cyclones in these three regions. For some winter TLEs over the Mediterranean Sea, the area surrounding Japan, and the east coast of North America, no midlatitude cyclone centers near the TLEs are identified from the SLP data using our method. Instead, the SLP values near the location of TLEs are lower than the surrounding grids. The incipient cyclones with cold front and warm front features are usually formed near the east coasts of the Asian continent and North America [*Eichler and Higgins*, 2006] and the western and southern coasts of the Mediterranean Sea [*Bocheva et al.*, 2007], and they then develop into mature cyclones while moving eastward. Therefore, it is possible that the midlatitude cyclones that induced the winter TLEs in the Pacific Ocean and the Atlantic Ocean are at the mature phase, so the SLP values of the storm centers are low enough to be easily identified. Therefore, it is likely that most of the winter TLEs recorded in the Mediterranean Sea, near Japan, and near the east coast of North America were induced by the cold front of the incipient cyclones, while their central pressures are *not* yet low enough to be identified using the previously prescribed method. Because of the smaller sea area of the Mediterranean Sea compared with the Pacific Ocean and Atlantic Ocean, the development and phase of midlatitude cyclones in the Mediterranean Sea may likely correspond to

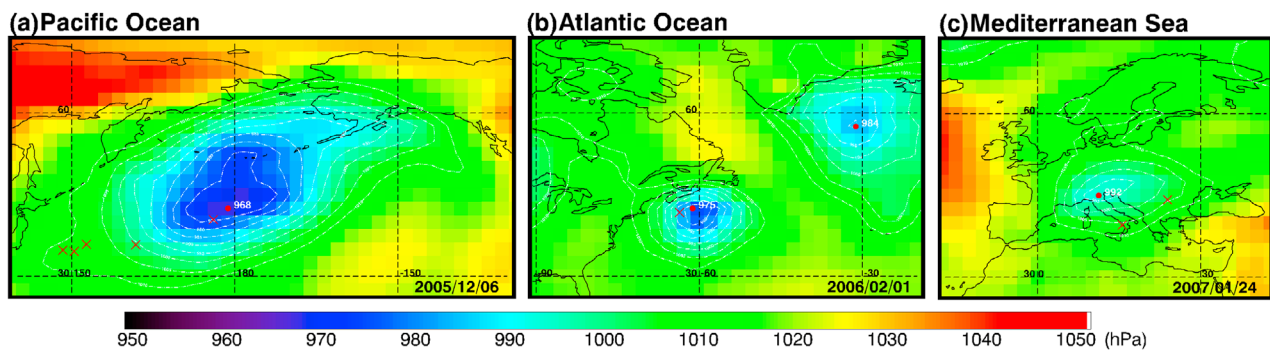


**Figure 6.** Representative occurrences of the northern winter TLEs near the midlatitude cyclones. Red crosses represent the locations of the TLEs, and red dots denote the centers of the midlatitude cyclones in (a) the Pacific Ocean on 6 December 2005, (b) the Atlantic Ocean on 1 February 2006, and (c) the Mediterranean Sea on 24 January 2007.

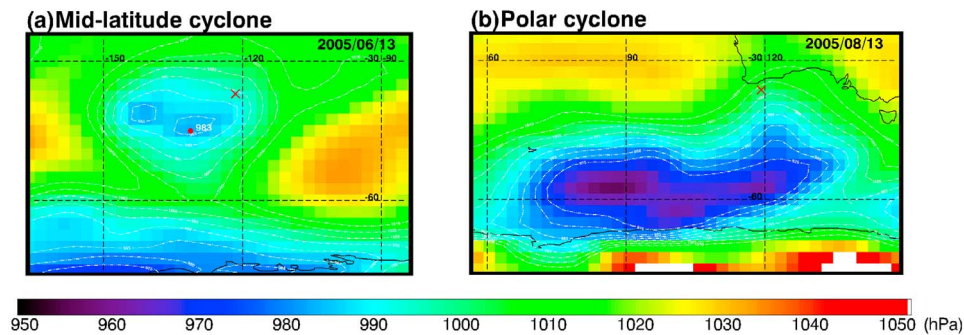


**Figure 7.** Occurrences of the southern winter TLEs near a midlatitude cyclone and a polar cyclone. Red crosses mark the locations of the TLEs, and red dots denote the centers of (a) the midlatitude cyclone on 13 June 2005 and (b) the polar cyclone on 13 August 2005.

those of the area surrounding Japan and the east coast of North America, where the cyclones are usually in the incipient phase. However, the winter TLEs can be produced either by the mature midlatitude cyclones or by the cold fronts of the incipient midlatitude cyclones; hence, the northern winter TLEs from both types of systems are included in this study. Through analyzing the distributions of 312 winter TLEs and the centers of the midlatitude cyclones, 88% of the ISUAL winter TLEs are found to be correlated with midlatitude cyclones for the northern winters.

[15] During the southern winters, the number of recorded winter TLEs is much less than that for the northern winters. The occurrence of the winter TLEs is distributed over the south and the east coasts of Australia, the South Pacific Ocean, and South America, but the distributions of southern winter TLEs are more scattered compared to the northern winter TLEs. Through correlating the daily winter TLEs with the SLP map, the results indicate that the winter TLEs are distributed not only around midlatitude cyclones but also around polar cyclones. Figures 7a and 7b show examples of winter TLEs occurring near the southern midlatitude cyclone and the polar cyclone. The midlatitude cyclones tend to converge into the polar cyclones and to develop from the instability of the polar cyclones, which rotate and move eastward around Antarctica. The southern winter TLEs cannot be correlated exactly with the midlatitude cyclone or the polar cyclone, so both systems are considered to be the generating systems of the southern winter TLEs. Through analyzing the distribution of 127 ISUAL southern winter TLEs, 72% of them are found to be correlated with the midlatitude cyclones or the polar cyclones. Most of the observed southern winter TLEs are located to the north of the cyclone centers; also the cold fronts are on the north side of the cyclones in contrast to those in the Northern Hemisphere. Therefore, the southern winter TLEs are presumably induced by the cold fronts of the midlatitude cyclones and the polar cyclones. Consequently, both the northern and the southern winter TLEs are associated with the cold fronts of the cyclones.

#### 4.2. Winter TLE Occurrence Density and Storm-Track Frequency

[16] The eastward moving path of the midlatitude cyclone is called the storm track, and the cumulative storm-passing times for a specific region over some time interval is the storm-track frequency. For a midlatitude cyclone, the typical

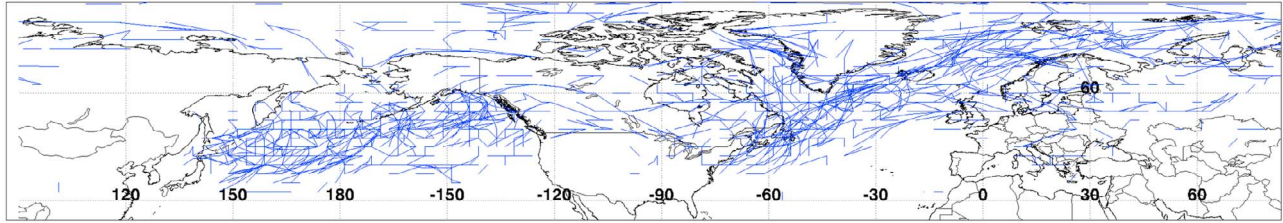
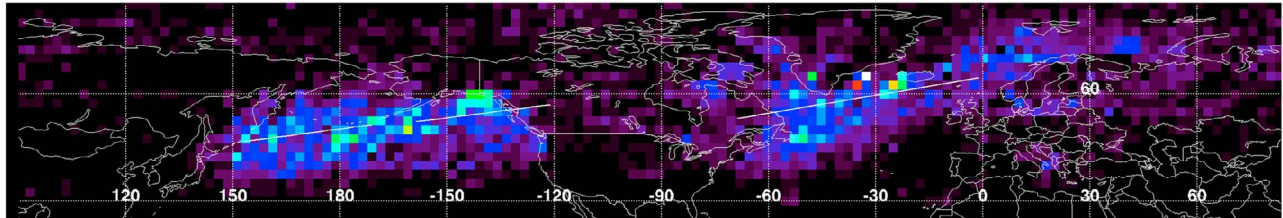
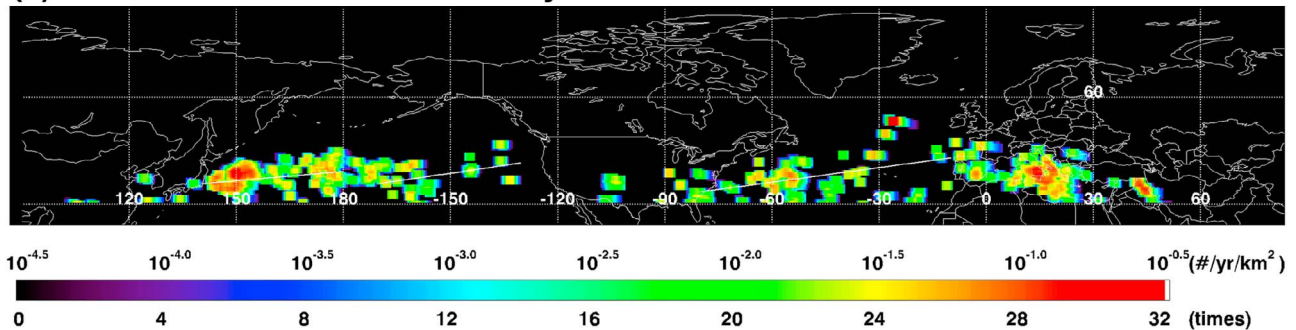
moving speed is lower than 133 km/h, and the distance traveled in a 6 hour interval thus is less than 800 km. If a storm center, which is identified from the 6 hour SLP data, moves less than 800 km in one step, then it counts as a single storm track, as shown in Figure 8a. The storm-track frequency for the Northern Hemisphere during the winters of 2004–2008 is shown in Figure 8b. Since the number of southern winter TLEs is small and the distribution is scattered, only the northern winter TLEs are analyzed in this section. The northern midlatitude region is subdivided into three regions for further discussions: the western Pacific Ocean (140°E–180°E), the eastern Pacific Ocean (190°E–230°E), and the Atlantic Ocean (280°E–350°E). We study the correlation of the winter TLE occurrence density (Figure 8c) and the storm-track frequency (Figure 8b).

[17] For the three northern subregions, both the storm-track frequency and the winter TLE occurrence density exhibit a lower left to the upper right distribution pattern. The white lines in Figures 8b and 8c represent the mean locations of the distributions. The mean locations of the winter TLE occurrence density for the three subregions are all located to the south of the storm-track frequency, with a 10°–15° offset. We believe that the strong shearing wind near the midlatitude cyclone center actually suppress the separation of charge, which in turn impedes the occurrence of lightning and TLEs. In addition, for midlatitude cyclone at the mature phase, the cold front can extend over 1000 km far from the center. During the cold fronts pushing southward at Japan and the Atlantic Ocean in the wintertime, the TLEs may be induced by the instability resulting from the polar air masses over the warmer water. Therefore, it is reasonable to have a distribution offset between the TLE occurrence density and the storm-track frequency.

[18] As it has been indicated in section 4.1, the winter TLEs are distributed around the cold front, which extends southward from the center of the midlatitude cyclone in the Northern Hemisphere. Therefore, it is expected that the mean locations of the winter TLE occurrence density should position to the south of that for the storm-track frequency.

#### 5. Luminous Intensities of the Tropical and Winter TLEs

[19] Analyses performed in section 4 have established the connection between the tropical TLEs and the ITCZ/SPCZ

**(a) Storm Tracks****(b) Storm-track Frequency****(c) Winter TLE Occurrence Density**

**Figure 8.** (a) Storm tracks, (b) storm-track frequency, and (c) the winter TLE occurrence density over 30°N–90°N in the northern winters from 2004 to 2008.

as well as the association of the winter TLEs with the mid-latitude cyclones. Hence, TLEs over the winter and the tropical regions are induced by different weather systems. In this section, we explore whether the brightness of the tropical and winter TLEs differs by comparing the luminous intensities of elves and sprites from the two domains.

### 5.1. Intensity of Elves

[20] For the elves occurring in front of the Earth's limb, ISUAL spectrophotometric data always contain a clear FUV emission peak or peaks [Chang *et al.*, 2010]. Chang *et al.* [2010] showed that the FUV emission in the ISUAL elves is from elves not lightning. Therefore, the elves' luminous intensity can be estimated from integrating its FUV emission. We analyze the in-front-of-the-limb elves that are 2500 to 2900 km away from the FORMOSAT-2 satellite and have luminous bodies that are fully inside the FOV of the ISUAL spectrophotometer/imager. Through Gaussian fitting of the FUV emission peak, the center and width of the emission peak can be extracted. To obtain the intensity, the FUV emission curve is divided into two parts. The first part of the photometric data embraces the emissions that are within two standard deviations from the center of the peak. The FUV emissions from two to nine standard deviations to the right of the peak are fitted to an exponentially decaying function.

The FUV intensity of an elve is the sum of the area under these two parts. The intensities are further normalized to a distance of 2500 km away from the FORMOSAT-2 satellite after correcting for the emission band contribution factor for the ISUAL spectrophotometer as described by Mende *et al.* [2005].

[21] There are 144 northern summer and 80 northern winter elves in the years of 2006 and 2007 that met the aforementioned conditions. Figures 9a and 9b are the distributions of the FUV intensity and the occurring latitude for these elves. The blue shaded and the red shaded regions denote the winter and the tropical domains, respectively. The data indicate that the FUV intensities of the 16 winter elves are all less than  $1.5 \times 10^4$  photons/cm<sup>2</sup>, while 20 of the 185 tropical elves have intensities that exceed  $1.5 \times 10^4$  photons/cm<sup>2</sup> and the highest is  $\sim 4.5 \times 10^4$  photons/cm<sup>2</sup>. The fraction of the tropical elves that has intensity exceeding  $1.5 \times 10^4$  photons/cm<sup>2</sup> is 20/185 ( $\sim 2/16$ ). If the germinating conditions for the winter elves are similar to their tropical counterparts, one or two winter elves with the luminous intensity exceeding  $1.5 \times 10^4$  photons/cm<sup>2</sup> would be expected, but none has been detected. Therefore, the convective systems in the tropical regions, which developed from the convergence of winds, likely are more capable of inducing bright elves. For the winter midlatitude regions, cold and warm

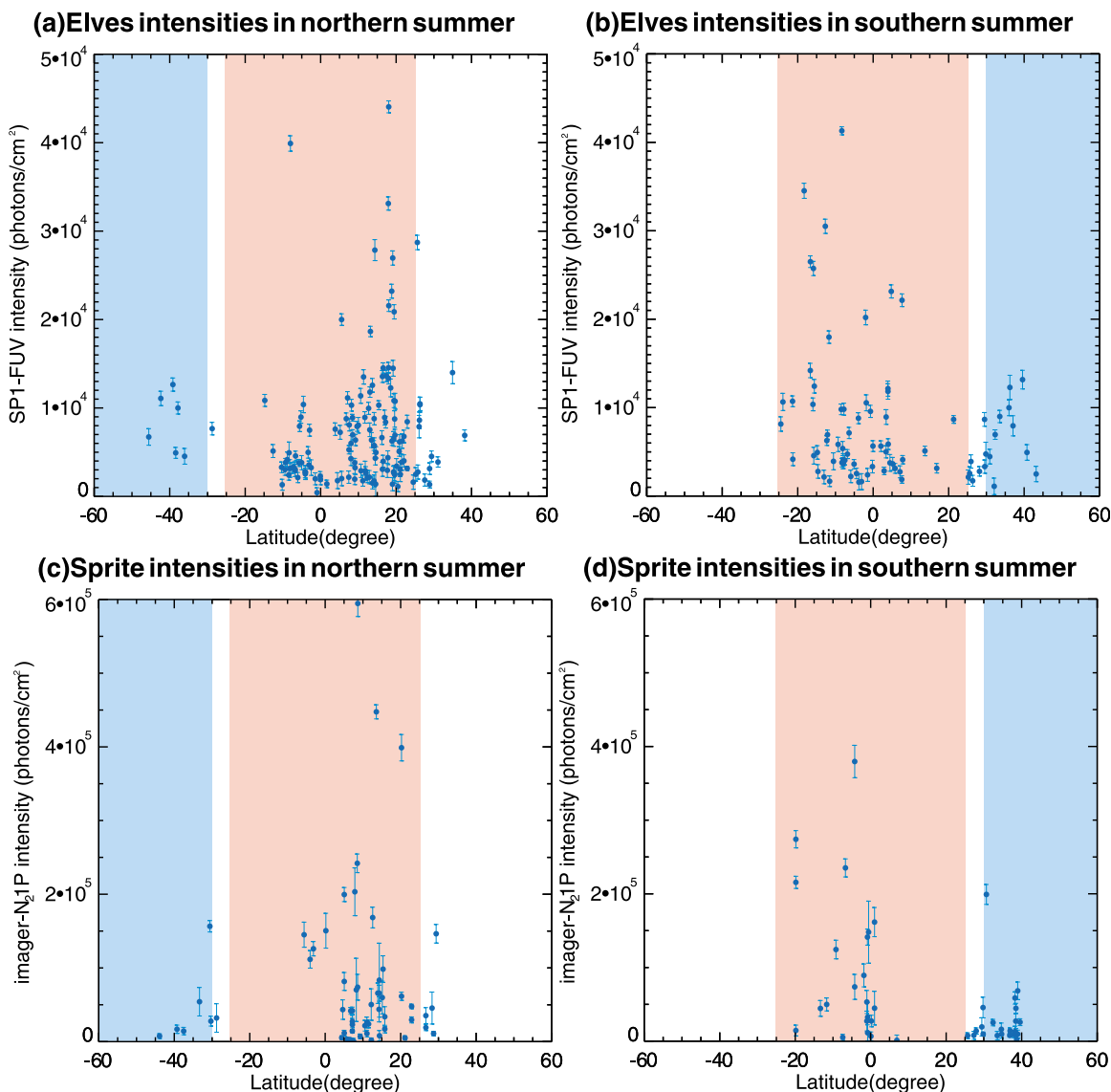


**Figure 9.** The occurrence latitudes and the luminous intensities for (a) the northern summer elves, (b) the northern winter elves, (c) the northern summer sprites, and (d) the northern winter sprites. Blue dots represent the elves or sprites. The red shaded and the blue shaded areas mark the low-latitude tropical and the winter midlatitude regions, respectively.

air masses of different properties collide, and the resulting uplifting convective systems can be formed at times; however, they may tend to induce low luminous elves.

## 5.2. Intensity of Sprites

[22] To infer the luminous intensity of sprites, events that are not contaminated by lightning emission and are fully inside of the FOV of the ISUAL imager are chosen. The intensity of sprites can be deduced through integrating the ISUAL imager  $N_21P$  data after the background is properly subtracted [Kuo *et al.*, 2008]. Sprites recorded during the northern summers and the northern winters for the years 2005–2008 are sampled. In all, 58 tropical sprites and 44 winter sprites conform to the selection conditions. Figures 9c and 9d show the imager- $N_21P$  intensities of sprites and their occurrence latitudes. The data indicate that the  $N_21P$  intensities of the 22 winter sprites are

all less than  $2 \times 10^5$  photons/cm<sup>2</sup>, while 10 of 68 tropical sprites have intensities that exceed  $2 \times 10^5$  photons/cm<sup>2</sup> with the highest being  $\sim 6 \times 10^5$  photons/cm<sup>2</sup>. The fraction of the tropical sprites that has intensity exceeding  $2 \times 10^5$  photons/cm<sup>2</sup> is 10/68 ( $\sim 3/22$ ). Therefore, a few winter sprites analyzed here should have intensities surpassing  $2 \times 10^5$  photons/cm<sup>2</sup> if their generating environments were similar to those of the tropical sprites, but none has. The results for the sprites are consistent with those for the elves; both point out that the tropical thunderstorm systems are presumably more capable of inducing bright TLEs than are their winter cousins.

## 6. Discussion and Summary

[23] The synoptic-scale factors that influence the distributions of TLEs over the tropical and the winter midlatitude

regions are deduced from ISUAL survey data. For the tropical regions, the ITCZ is the convergence zone of the Hadley cell, mainly formed from the convergence of the northeasterly trade wind and the southeasterly trade wind from each hemisphere. However, the distribution of ITCZ is not solely the result of the atmospheric latitudinal circulation; it is also influenced by the longitudinal circulation, the ocean currents, and the regional differences of the land-to-ocean ratio. Therefore, ITCZ at different longitudinal domains display variations in distribution and migration characteristics. Since TLEs are manifestations of deep convections, the ITCZ/SPCZ is expected to be the root factor that affects the tropical TLE distributions such that it would show regional variations matching that of the ITCZ/SPCZ. Indeed, 84% of TLEs occurred over the ITCZ/SPCZ, and the migrating characteristics of the TLE distributions in different longitudinal domains closely follow those of the ITCZ/SPCZ. For the midlatitude winter regions, the midlatitude cyclones are the most important weather systems and are perhaps the major weather system that contains sufficient energy and instability to invoke convective systems. Therefore, it is reasonable to expect that most of the winter TLEs are induced by the midlatitude cyclones. In fact, winter TLEs do often occur near the cold fronts extending from the midlatitude cyclone centers. The data show that 88% of the northern winter TLEs and 72% of the southern winter TLEs are related to the midlatitude cyclones, and the northern winter TLEs occur mainly in three areas: the Pacific Ocean, the Atlantic Ocean, and the Mediterranean Sea.

[24] The ITCZ, which is distributed over the tropical ocean and land, and the midlatitude cyclones, which are the dominant weather systems in the winter oceans and coasts, are the controlling synoptic-scale factors for the occurrence of the tropical and winter midlatitude TLEs. The distributions of the ISUAL TLEs show distinct band-like groupings. Since most of the TLEs are initiated by lightning, one has to ask whether the global lightning data exhibit such distribution patterns. With the guiding of the ISUAL TLE distributions, the groups in the OTD lightning data [Christian *et al.*, 2003] can be discerned but are not as apparent as that in the ISUAL TLE data. The reason for the banding features in the optical transient detector (OTD) data being less distinct is the  $\sim 10:1$  land-to-ocean lightning ratio. Hence, the tropical OTD data are dominated by the three lightning chimneys over the continents. Also, the winter lightning groups in OTD data appear as patches over the land, look like the extensions of the dominant continent lightning chimneys, and often are overlooked. For the ISUAL TLEs, the land/coast-to-ocean ratio is  $\sim 4:1$  for sprites,  $\sim 1:1$  for elves, and  $\sim 2:1$  for halos [Chen *et al.*, 2008]. Therefore, the tropical TLEs are distributed along bands that straddle the equator (Figures 1a and 1b). Also, the winter TLEs occur near the midlatitude cyclones that primarily rage over the coast/ocean and track eastward, thus forming easily recognizable bands on the global TLE distribution maps (Figures 1a and 1b). The lightning imaging sensor (LIS) lightning data [Petersen and Rutledge, 2001] contain nearly identical patterns as those in the OTD data for the tropical regions. Though for the winter midlatitude regions, the banding distributions of the lightning are even less apparent, since LIS/Tropical Rainfall Measuring Mission (TRMM) has a 35 orbital plane; thus a substantial portion of the midlatitude regions was not sur-

veyed. It should be noted that ISUAL lightning data also exhibit grouping features that are in-line with those in the ISUAL TLEs. However, detailed analyses of the ISUAL lightning data will be reported in a separate paper.

[25] Through comparing the luminous intensities for TLEs from the tropical and the winter regions, the tropical convective systems are found to be more capable of producing bright elves and sprites. Takahashi *et al.* [2003] and Yair *et al.* [2009] report that the winter thunderstorms in both Japan and the eastern Mediterranean were smaller in size with a lower cloud top height compared to the summer continental MCSs and the equatorial tropical storms. The winter sprites appeared as short and simple columns, or as carrots with a well-defined central body and a small number of branches and tendrils. Adachi *et al.* [2004] indicate that the number of sprite columns is proportional to the peak current intensity, while the vertical length of sprite columns is proportional to the charge moment. On the basis of the investigations in Japan and in Israel, we may conclude that the cloud top height and the horizontal shielding area of tropical thunderstorms are both higher and larger compared to those of the midlatitude winter thunderstorms. Also, the tropical thunderstorms may be able to cumulate more charges and have higher discharge heights. Hence, the tropical thunderstorms are more likely to produce lightning with large charge moments and peak currents, in turn, also more capable of initiating bright sprites and elves.

[26] From analyzing the distributions of ISUAL TLE data, the synoptic-scale factors that control the occurrence of TLEs are uncovered. For the low-latitude tropical regions ( $25^{\circ}\text{S} \sim 25^{\circ}\text{N}$ ), 84% of the TLEs were found to occur over the ITCZ/SPCZ, which are defined to be the regions having OLR values less than  $OLR_b$  ( $270 \text{ W/m}^2$ ) and  $\nabla \cdot \bar{V}_{200\text{hPa}}$  greater than 0. The distributions of ISUAL TLEs exhibited seasonal variations that migrate north and south with respect to the equator, in-line with those for the ITCZ [Waliser and Gautier, 1993]. For the midlatitude regions (latitudes beyond  $\pm 30^{\circ}$ ), the occurrence of TLEs congregated over the Pacific Ocean, the Atlantic Ocean, and the Mediterranean Sea during the winter seasons. Our study showed that 88% of the northern winter TLEs and 72% of the southern winter TLEs occurred near the midlatitude cyclones. The winter TLE occurrence density and the storm-track frequency share similar trends with the distribution of the winter TLEs offset by  $10^{\circ}$ – $15^{\circ}$ . This study also compared the luminous intensities of elves and sprites from the tropical and the winter midlatitude regions. The results show that the convective systems in the tropical regions tend to produce brighter TLEs compared with their winter midlatitude counterparts.

[27] **Acknowledgments.** Work was supported in part by the National Space Organization (NSPO) and National Science Council in Taiwan under grants 98-NSPO(B)-ISUAL-FA09-01, NSC98-2111-M-008-001-MY3, NSC97-2111-M-006-001-MY3, NSC96-2111-M-006-001-MY3, and NSC96-2112-M-006-003-MY3.

[28] Amitava Bhattacharjee thanks the reviewers for their assistance in evaluating this paper.

## References

- Adachi, T., H. Fukunishi, Y. Takahashi, and M. Sato (2004), Roles of the EMP and QE field in the generation of columniform sprites, *Geophys. Res. Lett.*, *31*, L04107, doi:10.1029/2003GL019081.

- Adachi, T., H. Fukunishi, Y. Takahashi, M. Sato, A. Ohkubo, and K. Yamamoto (2005), Characteristics of thunderstorm systems producing winter sprites in Japan, *J. Geophys. Res.*, *110*, D11203, doi:10.1029/2004JD005012.
- Bocheva, L., C. G. Georgiev, and P. Simeonov (2007), A climatic study of severe storms over Bulgaria produced by Mediterranean cyclones in 1990–2001 period, *Atmos. Res.*, *83*, 284–293, doi:10.1016/j.atmosres.2005.10.018.
- Chang, S. C., C. Kuo, L. Lee, A. B. Chen, H. Su, R. Hsu, H. U. Frey, S. B. Mende, Y. Takahashi, and L. Lee (2010), ISUAL far-ultraviolet events, elves, and the lightning current, *J. Geophys. Res.*, *115*(107), A00E46, doi:10.1029/2009JA014861.
- Chen, A. B., et al. (2008), Global distributions and occurrence rates of transient luminous events, *J. Geophys. Res.*, *113*, A08306, doi:10.1029/2008JA013101.
- Chern, J. L., R. R. Hsu, H. T. Su, S. B. Mende, H. Fukunishi, Y. Takahashi, and L. C. Lee (2003), Global survey of upper atmospheric transient luminous events on the ROCSAT-2 satellite, *J. Atmos. Sol. Terr. Phys.*, *65*, 647–659, doi:10.1016/S1364-6826(02)00317-6.
- Christian, H. J., et al. (2003), Global frequency and distribution of lightning as observed from space by the Optical Transient Detector, *J. Geophys. Res.*, *108*(D1), 4005, doi:10.1029/2002JD002347.
- Eichler, T., and W. Higgins (2006), Climatology and ENSO-related variability of North American extratropical cyclone activity, *J. Clim.*, *19*(10), 2076–2093, doi:10.1175/JCLI3725.1.
- Franz, R. C., R. J. Nemzek, and J. R. Winckler (1990), Television image of a large upward electrical discharge above a thunderstorm system, *Science*, *249*, 48–51, doi:10.1126/science.249.4964.48.
- Fukunishi, H., Y. Takahashi, M. Kubota, K. Sakanoi, U. S. Inan, and W. A. Lyons (1996), Elves: Lightning-induced transient luminous events in the lower ionosphere, *Geophys. Res. Lett.*, *23*, 2157–2160, doi:10.1029/96GL01979.
- Füllekrug, M. (2004), The contribution of intense lightning discharges to the global atmospheric electric circuit during April 1998, *J. Atmos. Sol. Terr. Phys.*, *66*, 1115–1119, doi:10.1016/j.jastp.2004.05.009.
- Ganot, M., Y. Yair, C. Price, B. Ziv, Y. Sherez, E. Greenberg, A. Devir, and R. Yaniv (2007), First detection of transient luminous events associated with winter thunderstorms in the eastern Mediterranean, *Geophys. Res. Lett.*, *34*, L12801, doi:10.1029/2007GL029258.
- Gu, G., and C. Zhang (2002), Cloud components of the Intertropical Convergence Zone, *J. Geophys. Res.*, *107*(D21), 4565, doi:10.1029/2002JD002089.
- Hardman, S. F., R. L. Dowden, J. B. Brundell, J. L. Bahr, Z. Kawasaki, and C. J. Rodger (2000), Sprite observations in the Northern Territory of Australia, *J. Geophys. Res.*, *105*, 4689–4697, doi:10.1029/1999JD900325.
- Hsu, R. R., H. T. Su, A. B. Chen, L. C. Lee, M. Asfur, C. Price, and Y. Yair (2003), Transient luminous events in the vicinity of Taiwan, *J. Atmos. Sol. Terr. Phys.*, *65*, 561–566, doi:10.1016/S1364-6826(02)00320-6.
- Hu, Y., D. Li, and J. Liu (2007), Abrupt seasonal variation of the ITCZ and the Hadley circulation, *Geophys. Res. Lett.*, *34*, L18814, doi:10.1029/2007GL030950.
- Kuo, C. L., A. B. Chen, J. K. Chou, L. Y. Tsai, R. R. Hsu, H. T. Su, H. U. Frey, S. B. Mende, Y. Takahashi, and L. C. Lee (2008), Radiative emission and energy deposition in transient luminous events, *J. Phys. D Appl. Phys.*, *41*, 234014, doi:10.1088/0022-3727/41/23/234014.
- Lyons, W. A. (1996), Sprite observations above the U.S. High Plains in relation to their parent thunderstorm systems, *J. Geophys. Res.*, *101*, 29,641–29,652, doi:10.1029/96JD01866.
- Mende, S. B., H. U. Frey, R. R. Hsu, H. T. Su, A. B. Chen, L. C. Lee, D. D. Sentman, Y. Takahashi, and H. Fukunishi (2005), D region ionization by lightning-induced electromagnetic pulses, *J. Geophys. Res.*, *110*, A11312, doi:10.1029/2005JA011064.
- Neubert, T., T. H. Allin, H. Stenbaek-Nielsen, and E. Blanc (2001), Sprites over Europe, *Geophys. Res. Lett.*, *28*, 3585–3588, doi:10.1029/2001GL013427.
- Ortęga, P., and T. Guignes (2007), Lightning activity analyses with respect to the SPCZ location, *Geophys. Res. Lett.*, *34*, L11807, doi:10.1029/2007GL029730.
- São Sabbas, F. T., and M. Saba (2008), Ground-based observations of sprites and other Transient Luminous Events in southern Brazil, *Eos Trans. AGU*, *89*(53), Fall Meet. Suppl., Abstract AE13A-0309.
- Sentman, D. D., E. M. Wescott, D. L. Osborne, D. L. Hampton, and M. J. Heavner (1995), Preliminary results from the Sprites94 aircraft campaign: 1. Red sprites, *Geophys. Res. Lett.*, *22*, 1205–1208, doi:10.1029/95GL00583.
- Serreze, M. C., F. Carse, R. G. Barry, and J. C. Rogers (1997), Icelandic low cyclone activity: Climatological features, linkages with the NAO, and relationships with recent changes in the Northern Hemisphere circulation, *J. Clim.*, *10*(3), 453–464, doi:10.1175/1520-0442(1997)010<0453:ILCACF>2.0.CO;2.
- Su, H.-T., R.-R. Hsu, A. B.-C. Chen, Y.-J. Lee, and L.-C. Lee (2002), Observation of sprites over the Asian continent and over oceans around Taiwan, *Geophys. Res. Lett.*, *29*(4), 1044, doi:10.1029/2001GL013737.
- Su, H. T., R. R. Hsu, A. B. Chen, Y. C. Wang, W. S. Hsiao, W. C. Lai, L. C. Lee, M. Sato, and H. Fukunishi (2003), Gigantic jets between a thundercloud and the ionosphere, *Nature*, *423*, 974–976, doi:10.1038/nature01759.
- Takahashi, Y., R. Miyasato, T. Adachi, K. Adachi, M. Sera, A. Uchida, and H. Fukunishi (2003), Activities of sprites and elves in the winter season, Japan, *J. Atmos. Sol. Terr. Phys.*, *65*, 551–560, doi:10.1016/S1364-6826(02)00330-9.
- Tsai, L. Y. (2008), Meteorological aspects of elves and jets, *Eos Trans. AGU*, *89*(53), Fall Meet. Suppl., Abstract AE13A-0303.
- van der Velde, O. A., W. A. Lyons, T. E. Nelson, S. A. Cummer, J. Li, and J. Bunnell (2007), Analysis of the first gigantic jet recorded over continental North America, *J. Geophys. Res.*, *112*, D20104, doi:10.1029/2007JD008575.
- Waliser, D. E., and C. Gautier (1993), A satellite-derived climatology of the ITCZ, *J. Clim.*, *6*(11), 2162–2174, doi:10.1175/1520-0442(1993)006<2162:ASDCOT>2.0.CO;2.
- Yair, Y., C. Price, M. Ganot, E. Greenberg, R. Yaniv, B. Ziv, Y. Sherez, A. Devir, J. Z. Bor, and G. Satori (2009), Optical observations of transient luminous events associated with winter thunderstorms near the coast of Israel, *Atmos. Res.*, *91*, 529–537, doi:10.1016/j.atmosres.2008.06.018.
- Yang, J., X. Qie, G. Zhang, Y. Zhao, and T. Zhang (2008), Red sprites over thunderstorms in the coast of Shandong Province, China, *Chin. Sci. Bull.*, *53*(7), 1079–1086, doi:10.1007/s11434-008-0141-8.
- Yano, H., S. Abe, and Y. Takahashi (2001), High-definition TV imagery of elves and sprites over the Mediterranean Sea during the 1999 Leonid meteor shower peak, paper presented at Asia-Pacific Radio Science Conference, Tokyo, 1–4 Aug.

S.-C. Chang, R.-R. Hsu, L.-J. Lee, and H.-T. Su, Department of Physics, National Cheng Kung University, Tainan 70101, Taiwan.

A. B. Chen, Institute of Space, Astrophysical and Plasma Sciences, National Cheng Kung University, Tainan 70101, Taiwan. (alfred@phys.ncku.edu.tw)

H. U. Frey and S. B. Mende, Space Sciences Laboratory, University of California, Berkeley, CA 94720, USA.

C.-L. Kuo and L.-C. Lee, Institute of Space Science, National Central University, Jhongli 32001, Taiwan.

P.-H. Lin and C.-C. Wu, Department of Atmospheric Sciences, National Taiwan University, Taipei 10617, Taiwan.

Y. Takahashi, Department of CosmoSciences, Hokkaido University, Sapporo 060-0808, Japan.